E-Cadherin Suppression Directs Cytoskeletal Rearrangement and Intraepithelial Tumor Cell Migration in 3D Human Skin Equivalents

Addy Alt-Holland[1], Yulia Shamis[1], Kathleen N. Riley[2], Teresa M. DesRochers[1], Norbert E. Fusenig[3], Ira M. Herman[2] and Jonathan A. Garlick[1]

The link between loss of cell–cell adhesion, the activation of cell migration, and the behavior of intraepithelial (IE) tumor cells during the early stages of skin cancer progression is not well understood. The current study characterized the migratory behavior of a squamous cell carcinoma cell line (HaCaT-II-4) upon E-cadherin suppression in both 2D, monolayer cultures and within human skin equivalents that mimic premalignant disease. The migratory behavior of tumor cells was first analyzed in 3D tissue context by developing a model that mimics transepithelial tumor cell migration. We show that loss of cell adhesion enabled migration of single, IE tumor cells between normal keratinocytes as a prerequisite for stromal invasion. To further understand this migratory behavior, E-cadherin-deficient cells were analyzed in 2D, monolayer cultures and displayed altered cytoarchitecture and enhanced membrane protrusive activity that was associated with circumferential actin organization and induction of the nonmuscle, β actin isoform. These features were associated with increased motility and random, individual cell migration in response to scrape-wounding. Thus, loss of E-cadherin-mediated adhesion led to the acquisition of phenotypic properties that augmented cell motility and directed the transition from the precancer to cancer in skin-like tissues.

Journal of Investigative Dermatology (2008) **128,** 2498–2507; doi:10.1038/jid.2008.102; published online 5 June 2008

INTRODUCTION

Squamous cell carcinoma (SCC) arises as a premalignant lesion of stratified squamous epithelium that is characterized by intraepithelial (IE) expansion of dysplastic cells (Dlugosz *et al.*, 2002). Following invasion, tumor cells migrate through the connective tissue through a dynamic modulation at the tumor cell–extracellular matrix (ECM) interface (Hotary *et al.*, 2006; Wolf *et al.*, 2007). SCCs tend to invade as single cells or as small cell clusters that have a greater tendency to metastasize than carcinomas that invade as large tumor cell masses. Although most studies have characterized the migratory behavior of single, invading cells as they encounter 3D ECM networks (Brabletz *et al.*, 2005; Hotary *et al.*, 2006; Gaggioli *et al.*, 2007), little is known about the dynamics of migration of SCC cells *within* a premalignant tissue before stromal invasion occurs. It is therefore important to further understand the migratory properties of IE tumor cells in precancerous lesions.

While changes in tissue architecture and loss of cell–cell adhesion are known morphological hallmarks of the IE stage of tumorigenesis, the role that alterations in intercellular adhesion play in the transition from IE neoplasia to early-stage invasive carcinoma remains unclear. It has been shown that loss of E-cadherin function is associated with advanced stages of SCC (Birchmeier and Behrens, 1994; Behrens, 1999; Conacci-Sorrell *et al.*, 2002) and is linked to tumor cell metastasis (Bissell and Radisky, 2001; Cavallaro and Christofori, 2004) and poor clinical prognosis in a variety of epithelial cancers (Bagutti *et al.*, 1998; Perl *et al.*, 1998). Loss of cell–cell adhesion due to the absence of E-cadherin function is associated with invasion and metastasis of SCC and an infiltrative pattern of single cell invasion. Although it has been thought that loss of E-cadherin was associated only with these later stages of tumorigenesis, identification of mutations in E-cadherin in premalignant breast and stomach have indicated that altered E-cadherin-mediated adhesion

[1]*Division of Cancer Biology and Tissue Engineering, Department of Oral and Maxillofacial Pathology, School of Dental Medicine Tufts University, Boston, Massachusetts, USA;* [2]*Cell and Molecular Physiology, School of Medicine, Tufts University, Boston, Massachusetts, USA and* [3]*German Cancer Research Center, Im Neuenheimer Feld 280, Heidelberg, Germany*

Correspondence: Dr Jonathan A. Garlick, Division of Cancer Biology and Tissue Engineering, School of Dental Medicine, Tufts University, South Cove building, Room 116, 55 Kneeland Street, Boston, Massachusetts 02111, USA. E-mail: jonathan.garlick@tufts.edu; Dr Addy Alt-Holland, Division of Cancer Biology and Tissue Engineering, Department of Oral and Maxillofacial Pathology, School of Dental Medicine, Tufts University, Boston, Massachusetts 02111, USA. E-mail: addy.alt_holland@tufts.edu and Dr Ira M. Herman, Department of Physiology, School of Medicine, Tufts University, Arnold building, 116 Harrison Avenue, Boston, Massachusetts 02111, USA. E-mail: Ira.herman@tufts.edu

Abbreviations: BM, basement membrane; ECM, extracellular matrix; HEK, human epidermal keratinocytes; IE, intraepithelial; SCC, squamous cell carcinoma; 3D, three dimensional

Received 14 December 2007; revised 25 February 2008; accepted 28 February 2008; published online 5 June 2008

may be involved in the early stages of carcinogenesis as well (Behrens, 1999). However, how loss of E-cadherin impacts on the IE stages of carcinoma progression and during the earliest transition from premalignancy to invasive carcinoma remains unclear.

In this study, we have explored the migratory properties of individual SCC cells upon loss of E-cadherin-mediated cell–cell adhesion. To elucidate how suppression of E-cadherin function impacts SCC cells motility, we first studied the migratory behavior of an SCC cell line (HaCaT-II-4) in 3D human tissue models that closely mimic the initial events in skin cancer progression. Using skin equivalent model that allowed the fate of IE tumor cells to be followed in the presence of epidermal keratinocytes, we observed that individual, E-cadherin-deficient cells undergo transepithelial migration as a prerequisite for their invasion into the underlying matrix. Analyzing the migratory behavior of these tumor cells in 2D cultures revealed that E-cadherin suppression was linked to the acquisition of motility structures, reorganization of the actin cytoskeleton, and induction of β actin. Collectively, these features are likely to contribute to the activation of the invasive tumor cell phenotype seen during the transition from precancer to carcinoma *in vivo*.

RESULTS

E-cadherin suppression is linked to IE tumor cell migration in 3D tissues

To determine whether loss of E-cadherin function was linked to a motile cell phenotype in 3D tissue context that mimicked premalignant disease, we developed a human skin equivalent model to directly monitor tumor cell migration within the epithelium. β-Gal-marked II-4 tumor cells were seeded on top of a preformed epithelium that was established 2 days earlier by seeding human epidermal keratinocytes (HEK) on type I collagen gels harboring dermal fibroblasts (Figure 1a) or on an acellular, human dermal substrate (AlloDerm) (Figure 1d). This sequential seeding of tumor cells on a layer of normal keratinocytes prevented the direct attachment of II-4 cells to the underlying connective tissue and allowed us to compare the migratory behavior of E-cadherin-competent and E-cadherin-deficient cells within the epithelium. Morphologic analysis of skin equivalents revealed that tissues harboring E-cadherin-competent, II-4 cells showed normal tissue architecture when grown on collagen gels (Figure 1b) or on AlloDerm (Figure 1e). Clusters of II-4 cells with altered morphology were seen in a suprabasal position (arrows) and no cells had separated from these clusters to spread between adjacent HEK. In contrast, tissues that harbored E-cadherin-deficient, H-2K^d-Ecad-II-4 cells revealed a disorganized architecture both on collagen gels (Figure 1c) and on AlloDerm (Figure 1f). Individual II-4 cells and small cell clusters appeared in the collagen gel (Figure 1c, arrows) and in the AlloDerm (Figure 1f, arrows) demonstrating that loss of E-cadherin function enabled tumor cells to migrate through the epithelium before invading into the underlying matrix. To determine the IE fate of tumor cells, tissue sections were double-immunostained with anti-β-Gal and anti-β-catenin antibodies (Figure 1g–j). Anti-β-catenin antibody identified cells either with normal distribution of β-catenin in adhesion-competent cells or with cytoplasmic β-catenin that provided evidence of loss of cell–cell adhesion in adhesion-deficient cells (Margulis *et al.*, 2005a). Clusters of β-Gal-marked, E-cadherin-competent cells (green) were restricted to the superficial layers of the epithelium when tissues were grown on collagen gels (Figure 1g, arrows) or on AlloDerm (Figure 1h, arrows) and similarly to the HEK, showed membrane localization of β-catenin (red) at cell–cell borders (Figure 1g and h). In contrast, individual, β-Gal-marked, E-cadherin-deficient cells (green) migrated through the epithelium (Figure 1i and j, arrowheads) and invaded into the underlying connective tissue (Figure 1i and j, arrows). In these cells, β-catenin was limited to the cytoplasm, where it colocalized with β-Gal (Figure 1i and j, yellow), confirming that migrating tumor cells were indeed E-cadherin deficient (Alt-Holland *et al.*, 2005). The ability to track the fate of single, motile IE tumor cells demonstrated that abrogation of cell–cell adhesion activated phenotypic changes that were a prerequisite for transepithelial tumor cell migration and invasion.

Loss of E-cadherin induces plasma membrane protrusions, cell scattering, and accelerated cell migration in 2D, monolayer cultures

To further understand the highly motile tumor cell phenotype that enabled transepithelial migration in 3D skin equivalents, the morphology and behavior of E-cadherin-competent and E-cadherin-deficient II-4 cells were analyzed in 2D, monolayer cultures. E-cadherin-competent cells formed well-organized colonies and showed fan-shaped lamellipodia that extended from cells at the periphery of colonies (Figure 2a and b, long arrows and insets). In contrast, E-cadherin-deficient cells migrated as single cells and exhibited extensive membrane ruffles, filopodia and unpolarized lamellipodia (Figure 2c, short arrows and inset). These findings demonstrated that E-cadherin suppression enabled cell scattering and increased plasma membrane protrusive activity.

To determine whether these features were linked to the migratory properties of E-cadherin-deficient II-4 cells, monolayer cultures were scrape-wounded and imaged immediately upon wounding and after 24 and 48 hours (Figure 3a–i). E-cadherin-competent, pBabe- (Figure 3a–c) and H-2K^d-EcadDC25-II-4 (Figure 3d–f) cells migrated slowly into the wound gaps that remained partly uncovered after 48 hours. In contrast, E-cadherin-deficient, H-2K^d-Ecad cells (Figure 3g–i) showed accelerated wound closure at 24 hours, and complete closure of the wound gap by 48 hours. When further quantified, E-cadherin-competent cultures showed an average of 40 and 70% wound closure 24 and 48 hours after wounding, respectively (Figure 3j), whereas loss of E-cadherin function resulted in augmented cell migration as seen by the 70% wound closure 24 hours after wounding and complete wound closure after 48 hours (Figure 3j).

The pattern of cell migration in response to scrape wounding injury was next analyzed by time-lapse video microscopy. E-cadherin-competent pBabe- (Figure 4a, and

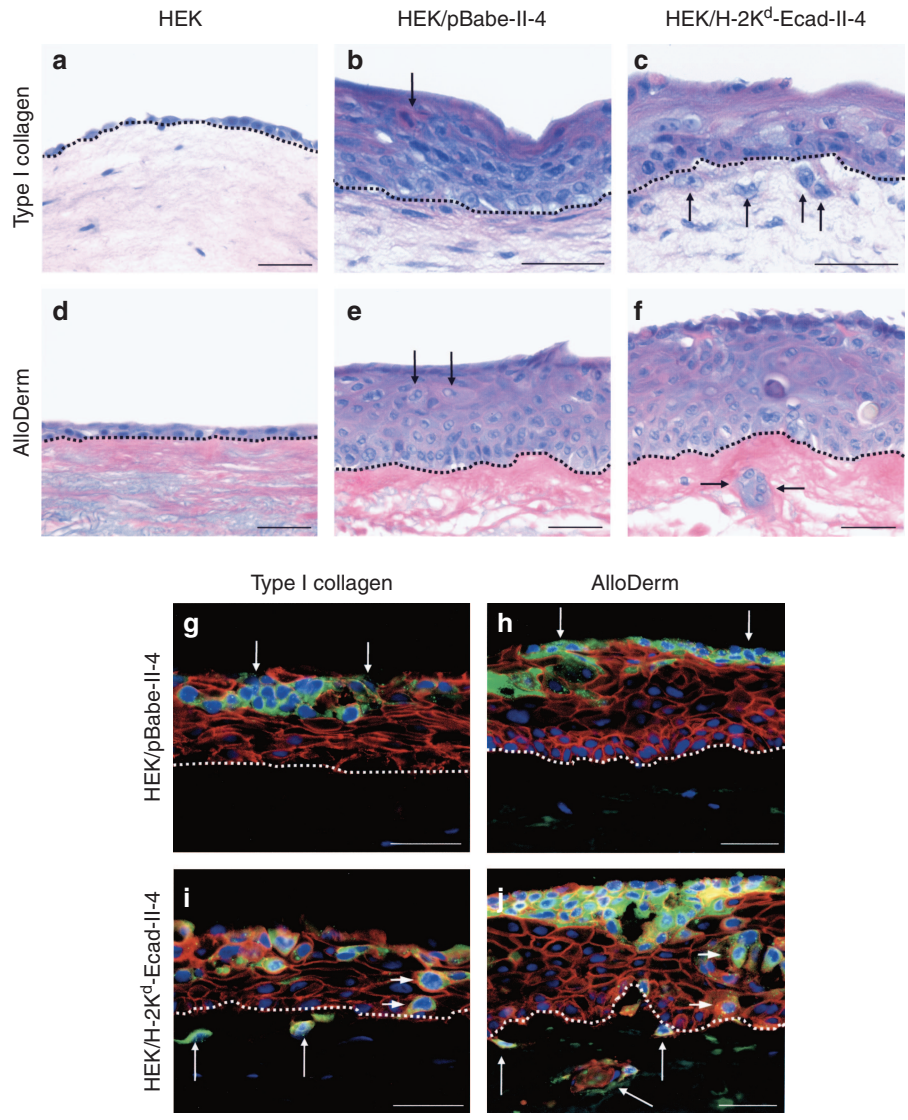

Figure 1. Abrogation of cell–cell adhesion results in transepithelial, individual migration of E-cadherin-deficient cells in 3D tissues. Morphology analysis of HEK following 2 days of growth showed formation of continuous cell layers on (**a**) contracted collagen gel or on (**d**) AlloDerm. Tissues generated by seeding β-Gal-positive, E-cadherin-competent pBabe-II-4 cells on top of HEK layers on (**b**) collagen or (**e**) AlloDerm showed organized architecture of basal and suprabasal layers and clusters of cells with aberrant morphology (arrows). Tissues generated by seeding β-Gal-positive, E-cadherin-deficient H-2K^d-Ecad-II-4 cells on top of HEK layers on (**c**) collagen or (**f**) AlloDerm demonstrated cells that had migrated into (**c**, arrows) the collagen or (**f**, arrows) the AlloDerm. Dashed line indicates the interface between the epithelium and the underlying matrix. Bar, 50 μm. Tissue sections were double-immunostained with anti-β-Gal (green) and anti-β-catenin (red) antibodies. (**g**, **h**) pBabe-II-4 cells were confined to superficial layers of the epithelium (arrows) and β-catenin was localized to cell–cell borders of HEK and pBabe-II-4 cells in tissues grown on (**g**) collagen or (**h**) AlloDerm. (**i**, **j**) H-2K^d-Ecad-II-4 cells had migrated between HEK layers (arrowheads) and invaded into (**i**, arrows) the collagen or (**j**, arrows) the AlloDerm. Whereas β-catenin was restricted to cell–cell borders of HEK, cytoplasmic colocalization of β-Gal and β-catenin was seen in H-2K^d-Ecad-II-4 cells (yellow). Dashed line indicates the interface between the epithelium and the underlying matrix. Bar, 50 μm.

Time-lapse movie S1) and H-2K^d-EcadDC25-II-4 cultures (data not shown, and Time-lapse movie S2) developed polarized lamellipodia at their leading edge that were oriented in the direction of the cell movement (Figure 4a, arrows). These cells migrated into the wound gap as a coherent cellular sheet while maintaining cell–cell adhesion. In contrast, E-cadherin suppression was linked to augmented motility of individual H-2K^d-Ecad-II-4 cells at the wound edge that demonstrated unpolarized and extensive membrane protrusions, elongated filopodia, and retraction fibers (Figure 4b arrows). These highly motile cells exhibited rapid, independent, and disoriented migration (Figure 4b, and Time-lapse movie S3). The pattern of migration of E-cadherin-competent and E-cadherin-deficient cells (colored asterisks, Figure 4a and b, marked cells) during the time-lapse video imaging was further analyzed utilizing computer-assisted cell-tracking measurements. E-cadherin-competent pBabe cells maintained their positions in relation to adjacent

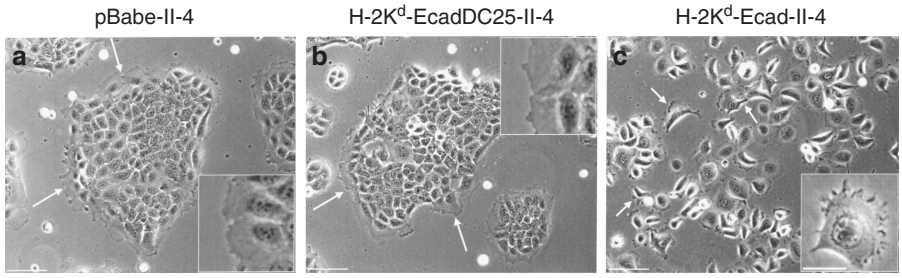

Figure 2. Loss of E-cadherin function is associated with single cell scattering. Phase-contrast images of (**a**) E-cadherin-competent pBabe, (**b**) H-2K^d-EcadC25-II-4, and (**c**) E-cadherin-deficient H-2K^d-Ecad-II-4 cultures. Note the fan-shape lamellipodia of pBabe- and H-2K^d-EcadC25-II-4 cells at the periphery of well-organized colonies (long arrows and insets) and the scattered H-2K^d-Ecad-II-4 cells that displayed extensive membrane ruffles, filopodia, and retraction fibers (short arrows and inset). Representative images are shown. Bar, 50 μm.

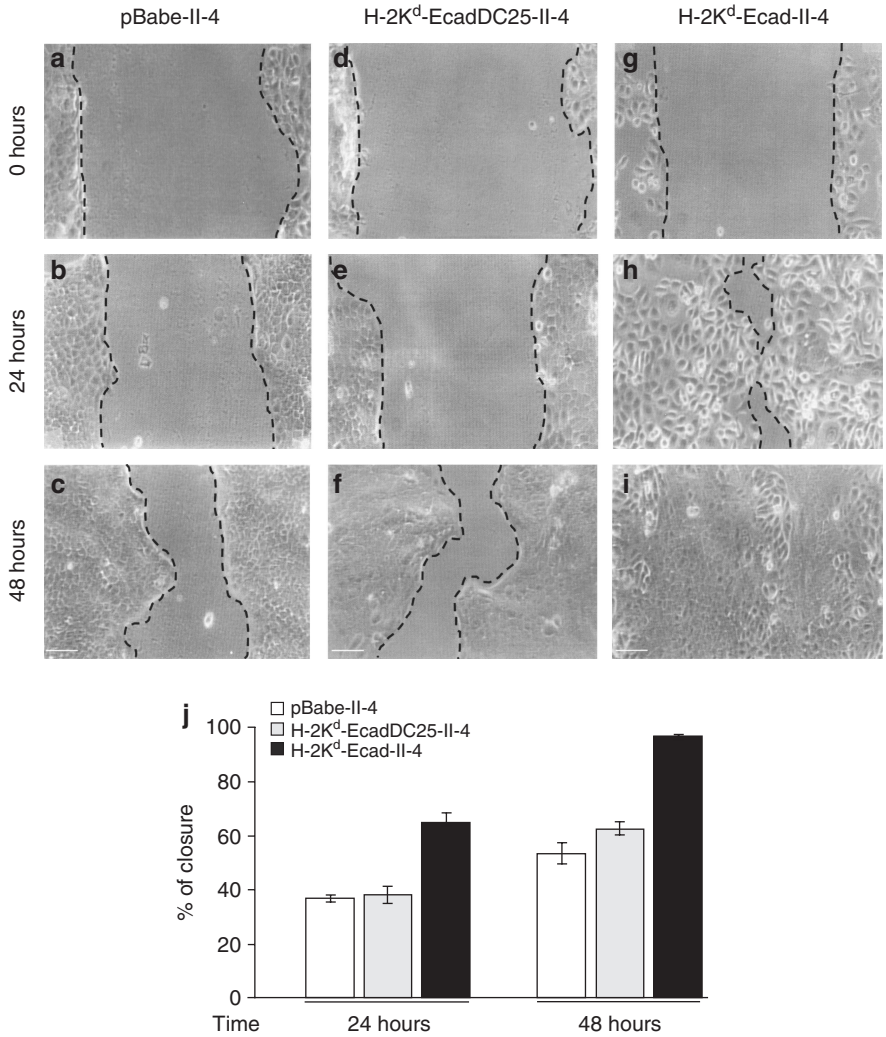

Figure 3. E-cadherin suppression is linked to accelerated wound closure in response to scrape-wounding *in vitro*. Phase contrast images of scrape-wounded (**a–c**) E-cadherin-competent pBabe and (**d–f**) H-2K^d-EcadC25-II-4 cultures, (**g–i**) and E-cadhrein-deficient H-2K^d-Ecad-II-4 culture at 0, 24, and 48 hours after wounding. Dashed lines indicate the edges of the wound gaps and demonstrate accelerated wound closure in H-2K^d-Ecad-II-4 culture. Bar, 200 μm. (**j**) The percentage of wound closure in pBabe (white), H-2K^d-EcadDC25 (gray) and H-2K^d-Ecad-II-4 (black) cultures at 24 and 48 hours was calculated relatively to the initial width of the wound gaps in the cultures. The mean ± SD of the width of the open wound gap was calculated in each of the indicated time points.

cells and showed directional cell migration (Figure 4c). In contrast, E-cadherin-deficient H-2K^d-Ecad cells showed random motility and decreased directionality as they migrated as individual cells into the wound gap (Figure 4c). In summary, these results showed that E-cadherin suppression was associated with increased plasma membrane protrusion activity that was linked to single cell scattering and random, augmented cell motility.

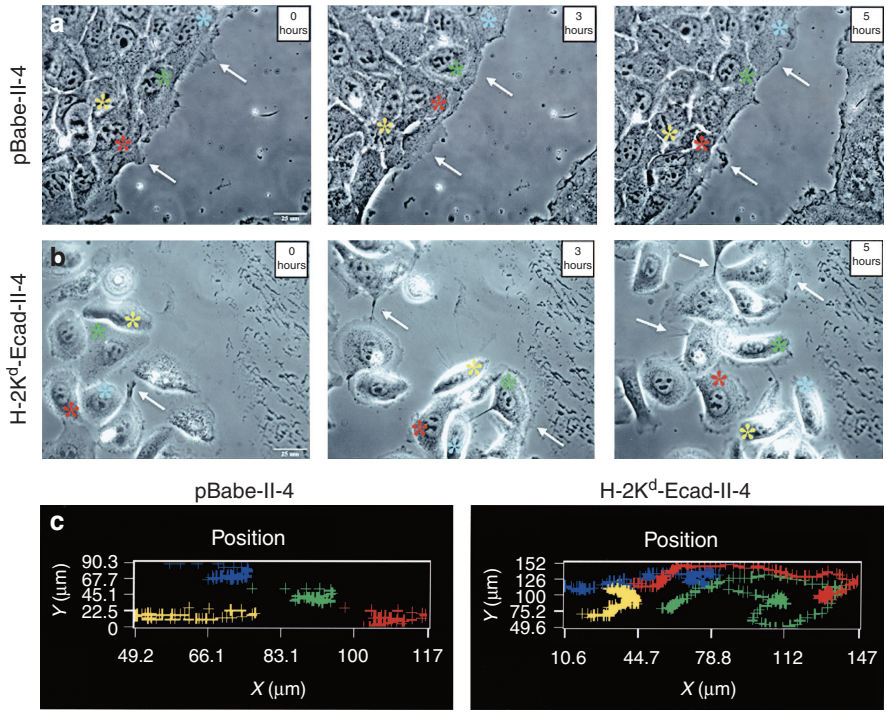

Figure 4. E-cadherin suppression is associated with independent, disoriented, and rapid cell migration. E-cadherin-competent pBabe- and E-cadherin-deficient H-2K^d-Ecad-II-4 cultures were grown on coverslides, and the cellular response to scrape-wounding injury was analyzed by time-lapse video microscopy, using phase-contrast microscope-imaging workstation. Representative video frames at the indicated time points are shown. Bar, 25 μm. (**a**) pBabe-II-4 cells at the wound edge displayed polarized morphology, developed lamellipodia at their leading edge (arrows), and demonstrated collective migration while maintaining their position within the monolayer. (**b**) Highly motile H-2K^d-Ecad-II-4 cells migrated randomly as single cells into the wound gap and displayed increased membrane protrusions and retraction fibers (arrows). (**c**) Graphic representation of cell tracking measurements show cell position and migration paths of four individual cells at the wound edge, marked by colored asterisks (marked cells in panels **a** and **b**), over the experiment time course. The position of the asterisk shows directional migration of pBabe-II-4 cells and indicates random migration of H-2K^d-Ecad-II-4 cells.

E-cadherin-deficient cells demonstrate circumferential, cortical actin organization, loss of actin stress fibers, and elevated β-actin expression

We next examined if actin cytoskeleton organization was altered in E-cadherin-deficient cells. E-cadherin-competent pBabe- and H-2K^d-EcadDC25-II-4 cells revealed a maze-like network of actin stress fibers between neighboring cells in well-organized colonies upon phalloidin staining (Figure 5a and b). Cells at the periphery of these colonies demonstrated perpendicular stress fibers that extended into lamellipodia (Figure 5a and b, arrows) and perimarginal actin bundles were axially aligned in adjacent cells (Figure 5a and b, arrowheads). In contrast, E-cadherin-deficient II-4 cells demonstrated circumferential, cortical actin (Figure 5c, arrows) and actin cables that extended into elongated filopodia (Figure 5c, arrowheads); however, no actin stress fibers were detected. These results showed that loss of cell–cell contact upon E-cadherin suppression was associated with actin cytoskeketon reorganization, loss of actin stress fibers, and extensive membrane protrusion activity that collectively contributed to the highly migratory phenotype of E-cadherin-deficient cells.

As nonmuscle, membrane-associated β actin localizes to regions of motile cytoplasm and plasma membrane protrusions during cell migration (DeNofrio *et al.*, 1989; Hoock *et al.*, 1991), we next studied its cellular distribution and possible contribution to the augmented migratory behavior of E-cadherin-deficient cells. Cultures of E-cadherin-competent and E-cadherin-deficient cells were grown on coverslides, scrape-wounded, and actin cytoskeleton and β actin were analyzed in migrating cells at the wound edge 7 hours later by immunofluorescence analysis. Phase-contrast images showed that migrating, E-cadherin-competent cells spread attenuated, fan-shaped lamellipodia into the wound gap (Figure 5d and e, arrows). These cells demonstrated actin stress fibers that extended toward the lamellipodia (Figure 5g and h, red) and a fine meshwork of β actin fibers that was intimately associated with the plasma membrane in lamellipodia and a short rim of filopodia at the leading edge of these cells (Figure 5g and h, green, arrows and insets). In addition, some of the actin stress fibers that extended toward the lamellae contained β actin-enriched domains along their length (Figure 5g and h, yellow). In contrast, migrating E-cadherin-deficient cells showed individual cells with extensive plasma membrane ruffling, elongated filopodia, and retraction fibers (Figure 5f, arrows). These cells demonstrated circumferential, cortical actin (Figure 5i, red) that contained β actin-enriched domains (Figure 5i, yellow), as well as intense β actin immunostaining throughout the cells and in regions of motile cytoplasm such as membrane

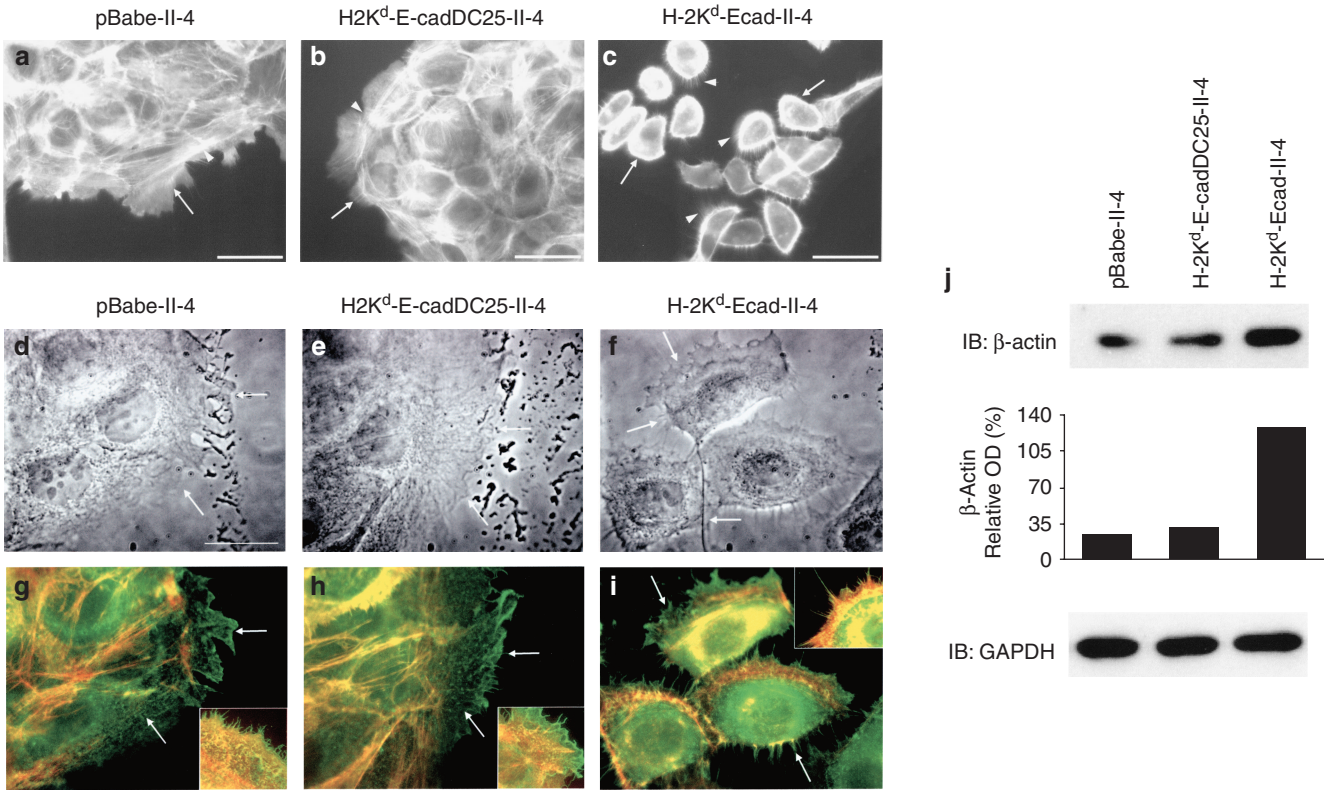

Figure 5. Loss of E-cadherin function is coordinated with actin cytoskeleton rearrangement and β actin induction. E-cadherin-competent- and E-cadherin-deficient cells were grown on coverslides, fixed and visualized by phalloidin. Colonies of (**a**) pBabe- and (**b**) H-2K^d-EcadDC25-II-4 cells showed an abundance of actin stress fibers between adjacent cells (arrowheads) and polarized lamellipodia (arrows), whereas (**c**) H-2K^d-Ecad-II-4 cells showed circumferential actin (arrows) and actin in filopodia and spikes (arrowheads). Representative micrographs are shown. Bar, 50 μm. Cultures were fixed 7 hours after scrape-wounding and double-stained with phalloidin (red) and anti-β actin antibodies (green). (**d–f**) Phase-contrast images of cells at the wound edge and (**g–i**) the respective immunofluorescence images of the same cells are shown. (**d** and **g**) pBabe- and (**e** and **h**) H-2K^d-EcadDC25-II-4 cells displayed β actin in lamellipodia (arrows) and in a rim of short filopodia (insets). (**f** and **i**) H-2K^d-Ecad-II-4 cells demonstrated intense β-actin staining throughout the cells, in membrane protrusions, elongated filopodia, and spikes (arrows and inset). Bar, 25 μm. (**j**) Western blot analysis of β actin level in equal protein samples of lysates from pBabe-, H-2K^d-EcadDC25-, and H-2K^d-Ecad-II-4 cell cultures (IB: β-actin). E-cadherin-deficient cells demonstrated a threefold increase in β-actin expression in comparison with E-cadherin-competent cells. Densitometry of the relative intensity of β actin in the presented immunoblot is shown. GAPDH blotting verified equal protein loading (IB: GAPDH). Representative data from five different experiments are shown.

protrusions, elongated filopodia, and narrow spikes (Figure 5i, green, arrows and inset). The increased intensity of β actin immunostaining in E-cadherin-deficient cells was further confirmed by western blot analysis of whole cell lysates using affinity-selected anti-β actin IgG antibody (Figure 5j). Immunoblotting and densitometry analysis revealed a threefold increase in β actin expression in E-cadherin-deficient cells, in comparison with its expression level in E-cadherin-competent cultures. Collectively, these results showed that E-cadherin suppression was linked to β actin induction, actin cytoskeleton reorganization, and enhanced plasma membrane protrusive activity that may contribute together to the augmented motility of E-cadherin-deficient tumor cells in 2D cultures and 3D tissues.

DISCUSSION

Tumor cell migration, invasion, and metastasis require the integration of proteolysis and remodeling of ECM that is linked to loss of cell–cell adhesion and acquisition of cell contractibility (Friedl and Wolf, 2003; Wolf *et al.*, 2007). Invasive tumor cells encounter networks of ECM proteins and activate proteases at their cell surface, localized at focal adhesion contacts and motility structures such as lamellae, pseudopodia, and invadopodia, to locally degrade these substrates as they migrate through them. In a similar way, premalignant cells initiate their invasion upon basement membrane (BM) degradation and transmigration through assembly of pseudopodia-like extensions (Hotary *et al.*, 2003, 2006). However, it remains unclear if similar mechanisms of cell migration are active *before* potentially malignant cells reach the BM interface, namely as they transit within the epithelium in premalignant tissues. To address this question, we have studied the migratory properties of IE tumor cells in 3D tissue models that mimic precancerous human skin, and we have found that E-cadherin-deficient cells acquire a profile of migratory properties that enables their transepithelial migration and ultimate invasion into the connective tissue.

We have characterized this migratory behavior using an early stage, SCC cell line (HaCaT-II-4) in which E-cadherin

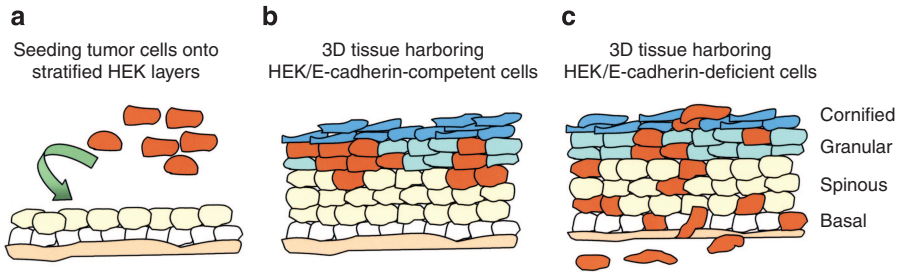

Figure 6. Transepithelial migration model of E-cadherin-deficient tumor cells in *in vivo*-like, 3D tissues during the transition from precancer to carcinoma. The schematic model proposes the occurrence of distinct stages of transmigration of E-cadherin-deficient tumor cells in the epithelium during the transition to early cancer cell invasion. (**a**) In this transepithelial migration model, E-cadherin-competent- or E-cadherin-deficient cells (designated in red) are seeded onto layers of stratified HEK. (**b**) When grown at an air–liquid interface, E-cadherin-competent cells are maintained in a dormant, suppressed state within the upper layers of the epithelium. (**c**) E-cadherin-deficient tumor cells separate from adjacent normal keratinocytes and undergo transepithelial, individual cell migration within the tissue, and attached to the BM, creating conditions that are permissive for invasion into the underlying stroma.

function has been disrupted by using a dominant-negative retroviral vector (Margulis *et al.*, 2005a). As a suppressor of invasiveness, loss of E-cadherin function is correlated with tumor cell invasion and poor clinical prognosis of a variety of cancers (Gumbiner, 2000; Thiery, 2002; Sun and Herrera, 2004). We demonstrated that loss of E-cadherin activated IE transmigration of individual II-4 cells between adjacent normal keratinocytes *before* their invasion into the underlying stroma. This migratory behavior was linked to assembly of motility structures including unpolarized lamellae and filopodia, actin cytoskeleton rearrangement, and β actin induction that resulted in individual, random cell scattering and augmented cell motility in 2D, monolayer cultures. These data provide a direct evidence that loss of E-cadherin function plays a critical role in activating the IE migration of SCC tumor cells during the transition from precancer to invasive SCC in a human skin-like tissue.

Stromal invasion of SCC cells occurs either as individual cell migration upon abrogation of cell–cell adhesion or by collective cell migration as cells maintain adhesive contacts and migrate as cohesive cellular sheets (Nabeshima *et al.*, 1999; Friedl and Wolf, 2003; Friedl *et al.*, 2004). As tumors spread from their primary site, they are thought to be linked to the dynamic modulation of tumor cell–ECM interfaces that they encounter following invasion. High-grade SCCs invade as single cells or as small clusters that have a greater tendency to metastasize than carcinomas that invade as large tumor cell masses with well-defined, pushing borders. Loss of cell–cell adhesion due to the absence of E-cadherin function is associated with an infiltrative pattern of single cell invasion. However, it remained unclear if loss of cell–cell adhesion in IE tumor cells activated pro-migratory properties that could direct tumor cell migration within a well-organized epithelium by spreading between adjacent epithelial cells *before* reaching the BM. We explored whether transepithelial migration in the context of a 3D, skin equivalent tissue was a critical step during this premalignant stage of tumor progression. To address this, we developed a 3D model for transepithelial migration of tumor cells that is schematically illustrated in Figure 6. The seeding of E-cadherin-competent or E-cadherin-deficient tumor cells onto a preformed epithelium prevented tumor cells from attaching directly to the underlying matrix and generated multilayered tissues in which tumor cells were initially found in a suprabasal position. To undergo invasion, IE tumor cells would be required to migrate as individual cells between normal surrounding keratinocytes to reach the BM. Their ability to do so indicated that the disruption of E-cadherin-mediated adhesion was associated with a shift from collective migration to migration of single, E-cadherin-deficient tumor cells in both 2D, monolayer cultures and within a multilayered epithelium. Interestingly, the collective migration of E-cadherin-competent cells in 2D cultures was similar to the compartmentalization and restricted migration of clusters of these cells in the superficial layers of the epithelium that prevented their ability to migrate between adjacent HEK.

Our results extend previous findings that matrix metalloproteinases direct degradation and migration through the BM upon assembly of invasive pseudopodial extensions (Hotary *et al.*, 2006), as we have previously shown that MMP-9 and MT1-MMP are elevated in E-cadherin-deficient-II-4 cells (Margulis *et al.*, 2005a, b). These proteases may also be active during transepithelial migration of IE tumor cells, as it has been shown that the transepithelial migration of dendritic cells is dependent on the MMP-9-mediated degradation of occludin in tight junctions (Ichiyasu *et al.*, 2004). Furthermore, the formation of filopodia and increased membrane protrusion activity seen upon loss of E-cadherin may also be linked to the ability of IE tumor cells to migrate through adjacent epithelia. A similar enhancement of membrane protrusions and peripheral pseudopodia has been reported upon loss of cell–cell adhesion and acquisition of migratory properties in Madin-Darby canine kidney (MDCK) cells (Behrens *et al.*, 1989) as well as upon invasion of SCC (Hotary *et al.*, 2006) and prostatic carcinoma cells (Partin *et al.*, 1988). Our results further substantiate that abrogation of E-cadherin-mediated adhesion and enhanced membrane protrusive activity act together to increase the migratory and invasive potential of E-cadherin-deficient carcinoma cells in both 2D cultures and 3D tissues.

Transepithelial tumor cell migration of II-4 cells appears to also be promoted by the dynamic reorganization of the actin cytoskeleton network upon loss of cell–cell adhesion. It has been shown that whereas γ actin isoform is mainly located in stress fibers, the β actin isoform is concentrated in regions of membrane ruffles and moving cytoplasm in nonmuscle cells (DeNofrio *et al.*, 1989; Rubenstein, 1990; Allen *et al.*, 1996). Herman and colleagues (DeNofrio *et al.*, 1989; Hoock *et al.*, 1991) have shown that β actin is found in a subset of membrane-associated cytoskeleton and is preferentially localized to motile regions of the plasma membrane at the leading edge of migrating microvascular pericytes, endothelial cells, and fibroblasts. In addition, highly motile MDCK cells showed both loss of actin stress fibers and increased β actin expression in multiple pseudopodia (Le *et al.*, 1998), whereas transformation of human fibroblasts *in vitro* resulted in expression of a mutant form of β actin and increased tumorigenicity *in vivo* (Leavitt *et al.*, 1982, 1987). We have extended these findings by demonstrating that loss of cell–cell adhesion can also induce β actin expression in association with the acquisition of migratory behavior in SCC cells. E-cadherin-deficient cells showed increased β actin expression and localization to areas of enhanced membrane protrusive activity that was orchestrated with actin cytoskeleton reorganization and loss of actin stress fibers. Our findings suggest that increased β actin expression and its association with plasma membrane protrusions may allow it to play a functional role in cell shape regulation and actin-based motility in E-cadherin-deficient II-4 cells. As it is known that loss of E-cadherin function triggers epithelial–mesenchymal transition (Thiery, 2002; Grunert *et al.*, 2003; Brabletz *et al.*, 2005; Margulis *et al.*, 2005b), it is intriguing to speculate that elevated levels of β actin in E-cadherin-deficient cells represent another characteristic of epithelial–mesenchymal transition-like behavior in highly migratory, epithelial tumor cells. Our study further substantiates these observations and shows that β actin induction, previously characterized in a variety of mesenchymal cell types, may also be linked to acquisition of mesenchymal properties in epithelial tumor cells upon loss of E-cadherin function.

The ability of IE tumor cells to transmigrate through an epithelium has important clinical implications for the recurrence of SCC at many primary sites. It has been theorized that multiple SCCs develop throughout the aerodigestive tract (''field cancerization'') as a result of widespread, IE migration of individual, tumor cells (van Oijen and Slootweg, 2000; Braakhuis *et al.*, 2003). As a consequence, broad areas of the epithelium are at an elevated risk for the development of premalignant lesions that can progress to malignancy (van Oijen and Slootweg, 2000; Braakhuis *et al.*, 2003). Our findings that highly migratory E-cadherin-deficient cells can spread laterally and vertically within tissues support the view that multiple SCCs seen in ''field cancerization'' may not develop independently of each other, but may rather be due to the IE migration of cells beyond the margins of the site of the primary lesion. By enabling individual cell migration within the epithelium, suppression of E-cadherin function may be an important risk marker for IE tumor cell migration that is linked to SCC recurrence.

Taken together, our results demonstrate that abrogation of E-cadherin-mediated adhesion induces augmented cell motility, actin cytoskeleton reorganization, and formation of active membrane protrusions and filopodia. These features are orchestrated to establish the transmigration of single tumor cells within epithelial tissues as a prerequisite for early SCC progression. Studying transepithelial migration in a biologically relevant, 3D human tissue now enables further studies to characterize mechanisms of incipient tumor cell invasion during the transition from precancer to malignancy. By exploring signaling pathways that regulate these events using *in vivo*-like human tissues, therapeutic approaches designed to block transepithelial tumor cell migration may pave the way toward elimination of such lesions and prevention of cancer development.

MATERIALS AND METHODS

2D, monolayer cell cultures

β-Gal-marked, HaCaT-II-4 keratinocytes (Boukamp *et al.*, 1990) were grown in DMEM containing 5% fetal bovine serum. Human dermal fibroblasts used for organotypic cultures were derived from newborn foreskins and grown in DMEM containing 10% fetal bovine serum. HEK were derived from newborn foreskins and grown on an irradiated 3T3 fibroblast feeder layer, in DMEM containing 10% fetal calf serum. Cells were grown at 37°C in 7.5% CO_2. E-cadherin-competent (pBabe and H-2K^d-EcadDC25) and E-cadherin-deficient (H-2K^d-Ecad) II-4 cells were generated by retroviral infection of HaCaT-II-4 cells as described previously (Margulis *et al.*, 2005a) (vectors provided courtesy of Dr. Fiona Watt). Studies carried out in this investigation were approved by the Institutional Review Board of Tufts University.

IE tumor cell migration in 3D tissue constructs

We generated 3D tissues that harbored mixtures of HEK and HaCaT-II-4 cells to explore IE tumor cell migration within these tissues. First, 6×10^5 HEK were seeded onto contracted type I collagen gel or onto human de-epidermalized dermis (AlloDerm, LifeCell Corp. Branchburg, NJ) placed on contracted collagen gel (Alt-Holland *et al.*, 2005). Cultures were maintained submerged for 2 days in low calcium epidermal growth medium to allow formation of an epithelial tissue that was 1–3 cell layers in thickness. This epithelial layer was generated to prevent tumor cells from attaching directly to the connective tissue interface. At that time, 1.5×10^5 β-Gal-marked, E-cadherin-competent (pBabe) or E-cadherin-deficient (H-2K^d-Ecad) II-4 cells were seeded onto the preformed HEK layers and cultures were submerged for additional 2 days in normal calcium epidermal growth medium and raised to an air–liquid interface for 5 days. In this way, IE tumor cell migration could be determined upon localization of β-Gal-expressing tumor cells present within the context of neighboring HEK. As II-4 cells were prevented from attaching to the connective tissue interface, the presence of β-gal-marked cells in the basal layer or the connective tissue would provide evidence of II-4 cell migration through the epithelium.

In vitro scrape-wounding and wound closure measurements

Cell cultures at 80% confluence were scrape-wounded using a 2–10 μl micropipette tip. Random areas along the wound gaps were

marked, photographed immediately upon wounding and 24 and 48 hours later. Wound closure measurements were based on the average change in the width of the wound gaps over time, relative to the initial width of the scrape-wounded gaps. For each culture, measurements were performed on three captured areas, and in each wounded area, 50–100 measurements of the wound gap were performed. In each time point, the mean ± SD of the width of the open wound gaps was calculated. To quantify wound closure over time, the averaged width of the open wound gaps at 24- and 48-hour time points were subtracted from the initial wound gaps measurements. This calculated measurement of wound closure was then divided by the initial width of the wound gaps to determine percentage of wound closure.

Time-lapse video microscopy and cell-tracking measurements

Cell cultures were grown on coverslides and scrape-wounded using a 2–10 µl micropipette tip. The coverslides were immediately mounted into a growth chamber with media and placed on 37°C, warmed microscope stage as reported previously (Young and Herman, 1985; DeNofrio *et al.*, 1989). Cell migration into the wound gaps was monitored using Axiovert 10 Zeiss microscope equipped with automated CCD camera (Hamamatsu Photonics, Japan). Image acquisition was performed at 5 minute intervals for 5 hours, using MetaMorph software 6.0 (Universal Imaging, Downingtown, PA). Cell position and migration paths were determined by tracking the nuclei positions of individual cells at the wound edge through the planes of each image stack, using MetaMorph software Track Point function.

Phase-contrast and fluorescence microscopy analysis

Phase-contrast images of cells were captured with PixeLINK Software 4.5 (Ottawa, ON, Canada), using inverted Axiovert 40C Zeiss microscope (Gottingen, Germany) equipped with PixeLINK Camera PL-A600 series (Ottawa, ON, Canada). For immunocytochemistry, cultures grown on coverslides were fixed with 4% paraformaldehyde in serum-free DMEM for 5 minutes. Cells were permeabilized for 90 seconds in lysis buffer (0.1% Triton-X, 50 mM HEPES, pH 7.1, 50 mM PIPES, pH 6.9, 1 mM $MgCl_2$, 0.5 mM EGTA, 75 mM KCl) and immunostained with affinity-purified rabbit anti-β actin IgG antibody (Hoock *et al.*, 1991) for 1 hour followed by rhodamine-conjugated phalloidin and Alexa 488-conjugated goat anti-rabbit secondary antibody (Molecular Probes, Eugene, OR) for 30 minutes at room temperature. For immunohistochemistry, tissues were frozen in embedding media in liquid nitrogen vapors and 6 µm serial sections were fixed in 4% paraformaldehyde and double-immunostained with mouse anti-β-catenin (Zymed, South San Francisco, CA) and rabbit anti-β-Gal (Cortex Biochem, San Leandro, CA) antibodies. Alexa 488-conjugated goat anti-rabbit and Alexa 594-conjugated goat anti-mouse were used as secondary antibodies. Tissue sections were counterstained with 4′-6-Diamidino-2-phenylindole (DAPI) in Vectashield mounting medium (Vector, Burlingame, CA). For tissue morphology, tissues were fixed in 10% formalin and embedded in paraffin, and hematoxylin and eosin staining was performed on 6 µm tissue sections. Immunofluorescent and hematoxylin and eosin images were captured with Spot Advanced Program 4.5, using a Nikon Eclipse 80*i* microscope (Nikon Instruments Inc., Melville, NY) equipped with a SPOT RT camera (Diagnostic Instruments, Sterling Heights, MI).

Western blot analysis

Cell cultures were extracted on ice with Radio Immuno Precipitation Assay (RIPA) buffer (150 mM NaCl, 50 mM Tris-HCl (pH 7.5), 10 mM EDTA, 1% Triton X-100, 10 mM NaF, 10 µg ml^{-1} aprotinin, 10 µg ml^{-1} leupeptin, 2 µg ml^{-1} pepstatin, 1 mM Phenylmethylsulfonylfluoride (PMSF), 200 µM $NaVO_4$). Protein concentrations were measured using bicinchoninic acid (BCA) Protein Assay Kit (PIERCE, Rockford, IL) and 5 µg protein samples were separated on 7.5% SDS-PAGE gel and transferred onto nitrocellulose membrane (Bio-Rad, Hercules, CA). The blot was probed with affinity-purified rabbit anti-β actin IgG antibody (Hoock *et al.*, 1991) followed by horseradish peroxidase-conjugated secondary antibody (Amersham, Piscataway, NJ). Membranes were stripped and reblotted with anti-GAPDH antibody (Abcam Inc., Cambridge, MA) followed by horseradish peroxidase-conjugated secondary antibody. Proteins were visualized using SuperSignal West Pico Chemiluminescent Substrate (PIERCE, Rockford, IL).

CONFLIFT OF INTEREST

The authors state no conflict of interest.

ACKNOWLEDGMENTS

We thank Jennifer Landmann for administrative assistance, Dr Mark W. Carlson for his helpful comments, and Adam Sowalsky for excellent technical assistance. We thank Dr F. Watt of the Imperial Cancer Research Center for the gift of the chimeric E-cadherin retroviral vectors. This work was supported by National Institutes of Dental and Carniofacial Research Grant no. 2RO1DE011250-06 (toJAG), and National Institutes of Health Grants EY-15125, GM-55110, and Healthpoint Inc. to IMH.

SUPPLEMENTARY MATERIAL

Time-lapse movie S1. Collective migration of E-cadherin-competent pBabe-II-4 cells in response to scrape-wounding in 2D culture.

Time-lapse movie S2. Collective migration of E-cadherin-competent H-2K^d-EcadDC25-II-4 cells in response to scrape-wounding in 2D culture.

Time-lapse movie S3. Individual, random migration of E-cadherin-deficient-H-2K^d-Ecad-II-4 cells in response to scrape-wounding in 2D culture.

REFERENCES

Allen PG, Shuster CB, Kas J, Chaponnier C, Janmey PA, Herman IM (1996) Phalloidin binding and rheological differences among actin isoforms. *Biochemistry* 35:14062–9

Alt-Holland A, Zhang W, Margulis A, Garlick JA (2005) Microenvironmental control of premalignant disease: the role of intercellular adhesion in the progression of squamous cell carcinoma. *Semin Cancer Biol* 15:84–96

Bagutti C, Speight PM, Watt FM (1998) Comparison of integrin, cadherin, and catenin expression in squamous cell carcinomas of the oral cavity. *J Pathol* 186:8–16

Behrens J (1999) Cadherins and catenins: role in signal transduction and tumor progression. *Cancer Metastasis Rev* 18:15–30

Behrens J, Mareel MM, Van Roy FM, Birchmeier W (1989) Dissecting tumor cell invasion: epithelial cells acquire invasive properties after the loss of uvomorulin-mediated cell–cell adhesion. *J Cell Biol* 108:2435–47

Birchmeier W, Behrens J (1994) Cadherin expression in carcinomas: role in the formation of cell junctions and the prevention of invasiveness. *Biochim Biophys Acta* 1198:11–26

Bissell MJ, Radisky D (2001) Putting tumours in context. *Nat Rev Cancer* 1:46–54

Boukamp P, Stanbridge EJ, Foo DY, Cerutti PA, Fusenig NE (1990) C-Ha-Ras oncogene expression in immortalized human keratinocytes (HaCaT) alters growth potential *in vivo* but lacks correlation with malignancy. *Cancer Res* 50:2840–7

Braakhuis BJ, Tabor MP, Kummer JA, Leemans CR, Brakenhoff RH (2003) A genetic explanation of slaughter's concept of field cancerization: evidence and clinical implications. *Cancer Res* 63:1727–30

Brabletz T, Jung A, Spaderna S, Hlubek F, Kirchner T (2005) Opinion: migrating cancer stem cells—an integrated concept of malignant tumour progression. *Nat Rev Cancer* 5:744–9

Cavallaro U, Christofori G (2004) Cell adhesion and signalling by cadherins and Ig-CAMs in cancer. *Nat Rev Cancer* 4:118–32

Conacci-Sorrell M, Zhurinsky J, Ben Ze'ev A (2002) The cadherin–catenin adhesion system in signaling and cancer. *J Clin Invest* 109:987–91

DeNofrio D, Hoock TC, Herman IM (1989) Functional sorting of actin isoforms in microvascular pericytes. *J Cell Biol* 109:191–202

Dlugosz A, Merlino G, Yuspa SH (2002) Progress in cutaneous cancer research. *J Investig Dermatol Symp Proc* 7:17–26

Friedl P, Hegerfeldt Y, Tusch M (2004) Collective cell migration in morphogenesis and cancer. *Int J Dev Biol* 48:441–9

Friedl P, Wolf K (2003) Tumour-cell invasion and migration: diversity and escape mechanisms. *Nat Rev Cancer* 3:362–74

Gaggioli C, Hooper S, Hidalgo-Carcedo C, Grosse R, Marshall JF, Harrington K *et al.* (2007) Fibroblast-led collective invasion of carcinoma cells with differing roles for rhogtpases in leading and following cells. *Nat Cell Biol* 9:1392–400

Grunert S, Jechlinger M, Beug H (2003) Diverse cellular and molecular mechanisms contribute to epithelial plasticity and metastasis. *Nat Rev Mol Cell Biol* 4:657–65

Gumbiner BM (2000) Regulation of cadherin adhesive activity. *J Cell Biol* 148:399–404

Hoock TC, Newcomb PM, Herman IM (1991) Beta actin and its MRNA are localized at the plasma membrane and the regions of moving cytoplasm during the cellular response to injury. *J Cell Biol* 112:653–64

Hotary K, Li XY, Allen E, Stevens SL, Weiss SJ (2006) A cancer cell metalloprotease triad regulates the basement membrane transmigration program. *Genes Dev* 20:2673–86

Hotary KB, Allen ED, Brooks PC, Datta NS, Long MW, Weiss SJ (2003) Membrane type I matrix metalloproteinase usurps tumor growth control imposed by the three-dimensional extracellular matrix. *Cell* 114:33–45

Ichiyasu H, McCormack JM, McCarthy KM, Dombkowski D, Preffer FI, Schneeberger EE (2004) Matrix metalloproteinase-9-deficient dendritic cells have impaired migration through tracheal epithelial tight junctions. *Am J Respir Cell Mol Biol* 30:761–70

Le PU, Nguyen TN, Drolet-Savoie P, Leclerc N, Nabi IR (1998) Increased beta-actin expression in an invasive moloney sarcoma virus-transformed MDCK cell variant concentrates to the tips of multiple pseudopodia. *Cancer Res* 58:1631–5

Leavitt J, Bushar G, Kakunaga T, Hamada H, Hirakawa T, Goldman D *et al.* (1982) Variations in expression of mutant beta actin accompanying incremental increases in human fibroblast tumorigenicity. *Cell* 28:259–68

Leavitt J, Ng SY, Varma M, Latter G, Burbeck S, Gunning P *et al.* (1987) Expression of transfected mutant beta-actin genes: transitions toward the stable tumorigenic state. *Mol Cell Biol* 7:2467–76

Margulis A, Zhang W, Alt-Holland A, Crawford HC, Fusenig NE, Garlick JA (2005a) E-cadherin suppression accelerates squamous cell carcinoma progression in three-dimensional, human tissue constructs. *Cancer Res* 65:1783–91

Margulis A, Zhang W, Alt-Holland A, Pawagi S, Prabhu P, Cao J *et al.* (2005b) Loss of intercellular adhesion activates a transition from low- to high-grade human squamous cell carcinoma. *Int J Cancer* 118:821–31

Nabeshima K, Inoue T, Shimao Y, Kataoka H, Koono M (1999) Cohort migration of carcinoma cells: differentiated colorectal carcinoma cells move as coherent cell clusters or sheets. *Histol Histopathol* 14:1183–97

Partin AW, Isaacs JT, Treiger B, Coffey DS (1988) Early cell motility changes associated with an increase in metastatic ability in rat prostatic cancer cells transfected with the V-Harvey-ras oncogene. *Cancer Res* 48:6050–3

Perl AK, Wilgenbus P, Dahl U, Semb H, Christofori G (1998) A causal role for E-cadherin in the transition from adenoma to carcinoma. *Nature* 392:190–3

Rubenstein PA (1990) The functional importance of multiple actin isoforms. *Bioessays* 12:309–15

Sun W, Herrera GA (2004) E-cadherin expression in invasive urothelial carcinoma. *Ann Diagn Pathol* 8:17–22

Thiery JP (2002) Epithelial–mesenchymal transitions in tumour progression. *Nat Rev Cancer* 2:442–54

van Oijen MG, Slootweg PJ (2000) Oral field cancerization: carcinogen-induced independent events or micrometastatic deposits? *Cancer Epidemiol Biomarkers Prev* 9:249–56

Wolf K, Wu YI, Liu Y, Geiger J, Tam E, Overall C *et al.* (2007) Multi-step pericellular proteolysis controls the transition from individual to collective cancer cell invasion. *Nat Cell Biol* 9:893–904

Young WC, Herman IM (1985) Extracellular matrix modulation of endothelial cell shape and motility following injury *in vitro*. *J Cell Sci* 73:19–32